International Journal of Advanced Smart Convergence Vol.9 No.2 58-67 (2020)
http://dx.doi.org/10.7236/IJASC.2020.9.2.58

IJASC 20-2-7

Data-Driven-Based Beam Selection for Hybrid Beamforming in Ultra-Dense Networks

Sang-Lim Ju,[1] Kyung-Seok Kim[2]

[1]*Doctor, Department of radio and communication engineering, Chungbuk National University, Korea*
[2]*Professor, Department of information and communication engineering, Chungbuk National University, Korea*
[1]*imaward@naver.com*, [2]*kseokkim@chungbuk.ac.kr*

Abstract

In this paper, we propose a data-driven-based beam selection scheme for massive multiple-input and multiple-output (MIMO) systems in ultra-dense networks (UDN), which is capable of addressing the problem of high computational cost of conventional coordinated beamforming approaches. We consider highly dense small-cell scenarios with more small cells than mobile stations, in the millimetre-wave band. The analog beam selection for hybrid beamforming is a key issue in realizing millimetre-wave UDN MIMO systems. To reduce the computation complexity for the analog beam selection, in this paper, two deep neural network models are used. The channel samples, channel gains, and radio frequency beamforming vectors between the access points and mobile stations are collected at the central/cloud unit that is connected to all the small-cell access points, and are used to train the networks. The proposed machine-learning-based scheme provides an approach for the effective implementation of massive MIMO system in UDN environment.

Keywords: *Coordinated beamforming, Data-Driven learning, MIMO, Machine-learning, Ultra-dense network*

1. Introduction

Wireless communication services have recently been expanding into various fields, including the internet of things (IoT), virtual reality applications, and machine-to-machine communication, in addition to the existing voice and data services. There are currently 1 billion cellular IoT connected devices in the world, with an expected 4.1 billions by 2024 [1]. Various studies have investigated ways to effectively accommodate the rapidly increasing mobile traffic [2–4]. Small cells and coordinated multi-point (CoMP) transmission and reception were introduced in fourth generation (4G) mobile communication [5, 6] as key technologies to handle this issue. These technologies allow multiple transmission nodes to increase their transmission capacity through coordinated signal processing.

New network technologies are needed in fifth generation (5G) mobile communication, to accommodate the

Manuscript Received: March. 28, 2020 / Revised: April. 2, 2020 / Accepted: April. 6, 2020
Corresponding Author: kseokkim@chungbuk.ac.kr(Kyung-Seok Kim)
Tel: +82-10-8802-5823
Professor, Department of information and communication engineering, Chungbuk National University, Korea

large data traffic in various cell types. Ultra-dense networks (UDNs) are being considered as a new network technology in which various small cell types can be deployed, with the number of small cells in the networks being greater than the number of active mobile stations (MSs) [4]. Because these small cells are being more densely deployed in 5G UDNs than in 4G heterogeneous networks, the separation between cells using the same frequencies is shortened. As a result, MSs are close to more cells than in a conventional network, and severe inter-cell interference may occur. Moreover, a UDN with a reduced cell radius can lead to frequent handovers caused by terminal mobility, which can greatly affect the performance of 5G communication systems. Additionally, in the directional communications in the millimetre-wave band considered in 5G, additional indirect handovers may occur because of obstacles. In CoMPs, all the decisions must be made at the central unit, based on the overall information on the network being reported in real time. Moreover, beam training massive multiple-input and multiple-output (MIMO) systems generates large overheads in beamforming [7]. Therefore, to implement massive MIMO systems in 5G UDN, an advanced, low-complexity coordinated beamforming (CB) scheme is required, to rapidly select a serving cell and the corresponding beamforming vector, and thus address both MS mobility and channel environment changes in real time.

Data-driven deep learning methods have shown excellent performance in various fields such as image classification, translation, and autonomous driving. In recent years, the application of machine learning to wireless communication systems has been studied using algorithms such as channel estimation [8] and hybrid precoding [9]. Machine-learning-based communication technologies can greatly reduce the time complexity of the involved algorithms. In this paper, we present an approach to integrate machine learning into the CB of massive MIMO systems in UDN contexts. We focus on achieving lower computational complexity and near-optimal performance compared to conventional methods [10] for the practical implementation of massive MIMO system in UDN. We have termed this machine-learning-based coordinated beamforming (ML-CB), consisting of two-stage deep neural network (DNN) models is capable of reducing the computational complexity required for CB in an environment with more deployed cells than MSs. Samples of the channel between the access unit (AU) of each small cell and an MS cell are obtained, and the optimal serving cell and best radio frequency (RF) beamforming vector are predicted by the DNN models, which has been trained to learn the relationship among channel samples, channel gain, and the results of conventional beam training. The performance of the proposed scheme is compared with that of the conventional approach, which finds the optimal solution by exhaustive search. The paper is organized as follows. In Section 2, the system model is described. Section 3 introduces the proposed ML-CB. The system performance as a function of the cell density in UDN and discussion are presented. Finally, Section 5 concludes the paper.

2. System model

We consider a millimetre-wave massive MIMO system based on 5G new radio (NR) access technology [11]. In this system, N_S AUs with a uniform rectangular array of N_t antennas, and one MS with N_r antennas are deployed in a highly dense arrangement of N_S small cells. The small cells are uniformly deployed, as in an urban micro cell scenario [12]. It is assumed that all the AUs are connected to a centralized/cloud processing unit (CU). The uplink pilot signal from an MS is received by all AUs, and the serving cell and RF beamforming vector for downlink data transmission are determined at the CU. In the downlink and uplink transmission operations, the modulation coding scheme and RF beamforming vector are determined for each resource block (RB). Therefore, in this study, we use a channel vector that averages a given channel matrix into 12 subcarriers per RB for system modelling. For a total of *K* RBs, the signal received from an MS by the *n*th AU, at the *k*th RB, $y_{n,k}$, can be written as

$$y_{n,k} = H_{n,k}^{u} u_{n,k} + \eta_{n,k}, \tag{1}$$

where $H_{n,k}^{u} \in \mathbb{C}^{N_r \times N_t}$ is a millimetre-wave channel as in [12], and the downlink channel $H_{n,k}$ can be estimated by exploiting the block sparsity of the channel matrix and channel reciprocity in time-division duplex mode [13]. In addition, $u_{n,k}$ is the uplink pilot signal, and $\eta_{n,k} \sim N_{\mathbb{C}}(0, \sigma^2)$ is the noise vector. The information related with $H_{n,k}$ is fed back from all AUs to the CU, and the serving cell and RF beamforming vector are then selected according to

$$\{n^*, i^*\} = arg \max_{\substack{w_i^{\mathrm{RF}} \in F_{\mathrm{RF}} \\ n \in N_S}} \left\| H_{n,k} w_i^{\mathrm{RF}} \right\|, \tag{2}$$

where $i = 1, \ldots, N_c^2$, N_c^2 being the length of the RF beamforming codebook, F_{RF}. The MS is therefore covered by the RF beam i^* from AU n^*, as per (2). The RF beamforming codebook is generated by a Kronecker-product of two discrete Fourier transform codebooks [14], one for each (vertical and horizontal) dimension. An RF beamforming codeword w_i^{RF} can be expressed as

$$\frac{1}{N_v}\left[e^{-j\phi(i)n_v}\right]_{n_v=0,\ldots,N_v-1} \otimes \frac{1}{N_h}\left[e^{-j\theta(i)n_h}\right]_{n_h=0,\ldots,N_h-1}, \tag{3}$$

where N_v and N_h are the number of antenna elements for the vertical and horizontal dimensions, respectively, and $\phi(i) = \frac{2\pi i}{N_c}$, $\theta(i) = \frac{2\pi i}{N_c}$ denote the zenith and azimuth angles of departure, respectively. The beam training required to select the serving cell and best RF beamforming vector at the CU increases as per $N_s \times K \times N_c^2$. Therefore, the overhead of beam training is greatly increased in environments with high small-cell density.

3. Data-driven-based Beam Selection

We propose a data-driven-based beam selection scheme to reduce the computational complexity of beam training in scenarios in which the density of small cells is much higher than that of the MSs. The conventional scheme to select a serving cell and the best beam according to (2) proceeds by exhaustive search. Even though achieving optimal performances, its overhead increases proportionally with the number of small cells. In contrast, the proposed scheme can only achieve performances close to those of the conventional method but does so with lower computational complexity.

The proposed ML-CB scheme consists of two steps and uses two DNNs for low complexity. In the first step, the channel gains between the MS and the AUs of all the small cells are predicted by a DNN regressor at the CU, and the small cell with the largest predicted channel gain is determined. When the MS is moving in environments with densely deployed small cells, the first stage approach is also required for low latency cell switching. In the second step, a DNN classifier determines the best RF beamforming vector to the MS from the best serving AU (determined in the first stage).

3.1 Training Dataset Representation in the First-Stage

3.1.1 Preprocessing of the Training Dataset

To construct effective models for both the DNN regressor and the DNN classifier, a large training data set is required. In the first step, we randomly deploy a large number of AUs and MSs L times and obtain all the

complex channel samples among them. DNNs cannot use complex training data, because their weights and biases are real-valued. It is therefore necessary to separate the complex channels into their real and imaginary components. We represent every column $h_{n,k,l}^{i}, i = 1, \ldots, N_t$ of the complex channel vector $H_{n,k,l}$ by its two components, $\Re\{h_{n,k,l}^{i}\}$ and $\Im\{h_{n,k,l}^{i}\}$. $H_{n,k,l}$ can hence be represented by $R_m \in \mathbb{C}^{1\times 2N_t}$, and be expressed as

$$R_m = \left[\Re\{h_m^1\}, \Im\{h_m^1\}, \ldots, \Re\{h_m^{N_t}\}, \Im\{h_m^{N_t}\}\right], \quad m = 1, \ldots, n \cdot k \cdot l, \ldots, N_L, \tag{4}$$

where $N_L = N_S \times K \times L \times N_r$ denotes the number of collected channel samples.

Millimetre-wave channels have a wide range of channel coefficients because of their frequency-selective fading, line-of-sight, and non-line-of-sight characteristics. Standardizing these parameters allows the DNN to correctly learn the channel characteristics from the samples. This is important for millimetre-wave massive MIMO systems, in particular. The training dataset $\mathcal{R}$ consists of only the real components and is expressed as $\mathcal{R} = \left[R_1, \ldots, R_{N_L}\right]^T$. Moreover, the *i*th column of $\mathcal{R}$ is expressed as $r_i = \left[\Re\{h_i^1\}, \ldots, \Re\{h_i^{N_L}\}\right]^T$, $r_i \in \mathbb{C}^{N_L\times 1}$, $i = 1, \ldots, 2N_t$. Every column of $\mathcal{R}$ is standardized as follows:

$$d_{\mathcal{R}}^{i} = \frac{r_i - \overline{r_i}}{\sigma(r_i)}, d_{\mathcal{R}}^{i} \in \mathbb{C}^{N_L\times 1}, \tag{5}$$

where $\overline{r_i}$ and $\sigma(r_i)$ denote the mean value and standard deviation of r_i, respectively. Consequently, the preprocessed training dataset $D_R \in \mathbb{C}^{N_L\times 2N_t}$ is given by

$$D_{\mathcal{R}} = \left[d_{\mathcal{R}}^{1}, \ldots, d_{\mathcal{R}}^{2N_t}\right] = \left[D_{\mathcal{R}}^{1}, \ldots, D_{\mathcal{R}}^{N_L}\right]^T. \tag{6}$$

3.1.2 Label Design

When using DNN models for communication, the training data labels will typically involve key performance indicators (KPIs) such as spectral efficiency, bit error rate, received signal power, and channel gain. We use channel gain as the KPI in the first stage. The serving cell selection approach using a channel gain criterion is the simplest approach to CB. When $D_{\mathcal{R}}^{i}$ is the *i*th row vector of a $D_{\mathcal{R}}$ matrix, the channel gain C_i of channel $D_{\mathcal{R}}^{i}$ can be expressed as $C_i = \left\|D_{\mathcal{R}}^{i}\right\|^2$. This value is used as the label for training data $D_{\mathcal{R}}^{i}$. The label C corresponding to $D_{\mathcal{R}}$ is expressed as $C = \left[C_1, \ldots, C_{N_L}\right]^T$. The DNN regressor predicts continuous quantities $\hat{C}$ for the test dataset.

3.2 Training Dataset Representation in the Second-stage

3.2.1 Preprocessing of the Training Dataset

In this stage, channel samples are generated as in the first stage, and the RF beamforming codebook given by (3) is used as raw data for training the DNN classifier. The RF beamforming vector $w_{\mathrm{i}}^{\mathrm{RF}}$, which is a complex vector, is also separated into real and imaginary components. The millimetre channels and the RF beamforming codebook are normalized with (5), so that the same criteria can be used when training. Consequently, the preprocessed training dataset, $D_C \in \mathbb{C}^{\left(N_c^2+N_L\right)\times 2N_t}$ is given by

Table 1. Label design in the classifier model.

RF BF vector	Integer	One-hot encoding	Length of encoded

	encoding	vector
w_0^{RF}	1	1 0 0 0 0 ⋯ 0 0 0 0
w_1^{RF}	2	0 1 0 0 0 ⋯ 0 0 0 0
⋮	⋮	⋮ N_c^2
$w_{N_c^2-2}^{\mathrm{RF}}$	N_c^2-1	0 0 0 0 0 ⋯ 0 0 1 0
$w_{N_c^2-1}^{\mathrm{RF}}$	N_c^2	0 0 0 0 0 ⋯ 0 0 0 1

$$D_C = \left[d_C^1, \ldots, d_C^{N_c^2}, d_C^{N_c^2+1}, \ldots, d_C^{N_c^2+N_L}\right]^T, \tag{7}$$

where the vectors d_C^1 to $d_C^{N_c^2}$ denote the preprocessed RF beamforming codebook training data, and the vectors $d_C^{N_c^2+1}$ to $d_C^{N_c^2+N_L}$ denote the preprocessed training channel samples.

3.2.2 Label Design

The label in the second stage is designed to classify RF beams highly correlated with the channels, i.e. a training dataset. First, conventional CB [15] is performed with the channel samples using (2), and an RF beamforming vector highly correlated with each channel sample is selected. Each RF beamforming vector denotes a unique class; an integer value is assigned to each RF beamforming vector, to allow the DNN classifier to classify the RF beam corresponding to each channel sample. The second column of Table 1 shows the assigned integers. Next, one-hot encoding is used to represent the integer value, as shown in the third column in Table 1. The length of the one-hot encoding vector is N_c^2, which is equal to the number of classes. The label $\mathcal{I}$ corresponding to D_C is expressed as follows: $\mathcal{I} = \left[\mathcal{I}_1, \ldots, \mathcal{I}_{N_L}\right]^T$. The DNN classifier predicts all the labels $\hat{\mathcal{I}}$ for the test dataset.

3.3 Building the Neural Networks

In this section, we describe how to build the DNN regressor and DNN classifier models, and train them with the training datasets $D_{\mathcal{R}}$, D_C, C, and $\mathcal{I}$ described in the previous sections. Our focus in this study is on the use of machine learning for CB with the context of 5G UDN implementation, not on the development or optimization of neural networks. Therefore, uncomplicated DNN models are used in the proposed ML-CB system. DNNs of this paper were built using the best performing network architecture as determined from experiments. Both the regressor and classifier models consist of five hidden dense layers. Each hidden layer uses the rectifier linear unit activation function. The optimizer uses the Adam method, which considers both gradient and learning rate, and is not affected by the rescaling of the gradient [16]. The batch size was 200, and the regressor and classifier models were trained with 10,000 and 1,000 iterations, respectively. The two DNN models have different structures in the output layer (OL) and compiler, because of their specific tasks. The regressor model has one node in the OL to predict the label of the test data. The mean-squared error (MSE) is used as the loss function in the compiler. It is defined as

$$\mathcal{L}_{\mathrm{MSE}} = \frac{1}{N_L}\sum_{i=1}^{N_L}\left(C_i - \hat{C}_i\right)^2. \tag{8}$$

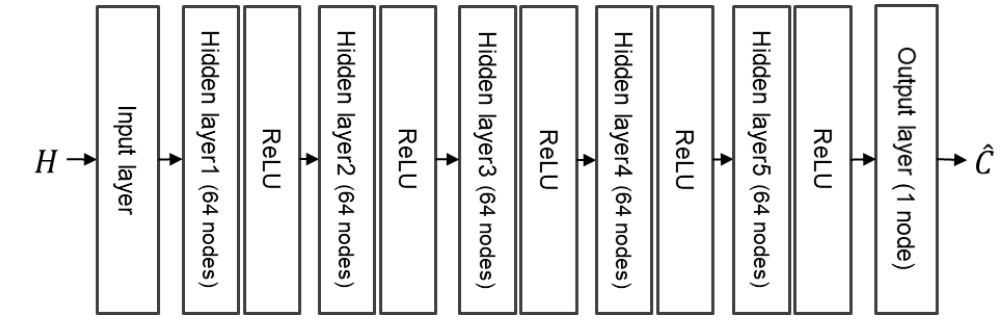

(a) DNN regressor model configuration

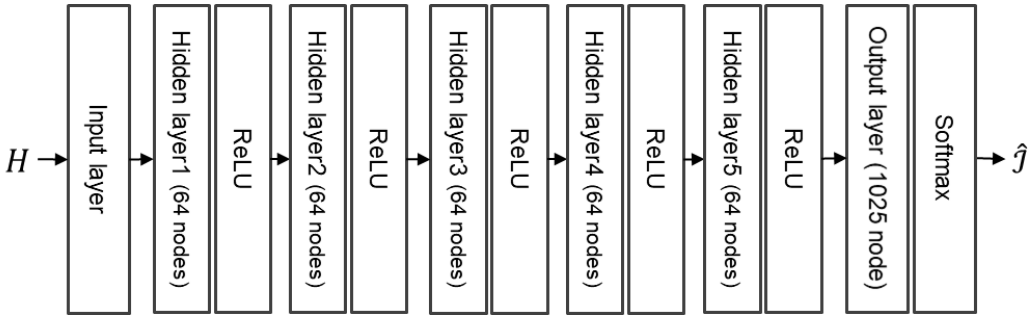

(b) DNN classifier model configuration

Figure 1. Proposed DNN model configurations.

The regressor model is trained to minimize $\mathcal{L}_{\mathrm{MSE}}$. The number of nodes in the OL of the classifier model is the same as the number of classes, and softmax activation is used. The categorical cross-entropy is used as a loss function in the compiler. It is defined as

$$\mathcal{L}_{\mathrm{CCE}} = -\sum_{i=1}^{N_c^2}\left(\hat{J}_i * log(\mathcal{F}(s)_i)\right), \tag{9}$$

where $\mathcal{F}(s)_i$ denotes the softmax function, s is the output score, and $\mathcal{F}(s)_i = e^{s_i}/\sum_j^{N_c^2} e^{s_j}$. A smaller value for $\mathcal{L}_{\mathrm{CCE}}$ means that $\hat{J}_i$ is more similar to the matching label. The detail configuration for two DNN models is shown as Fig. 1.

3.4 Operation of the ML-CB-based Massive MIMO System

In the proposed system, the regressor and classifier models learn from the training datasets described above, optimizing their weights. The optimized DNN models and weights are stored at the CU. In a network of dense small cells and one MS, the estimated downlink channel information in $y_{n,k}$ is fed back to the CU. The serving cell is determined by the trained regressor model after preprocessing the test data. The channel information between the serving cell and the MS is extracted, and the best RF beamforming vector is then determined by the trained classifier model. The CU transmits the hybrid precoding matrix processed by the selected beamforming vector to the AU of the selected serving cell, and the downlink transmission operation is performed by the designated AU.

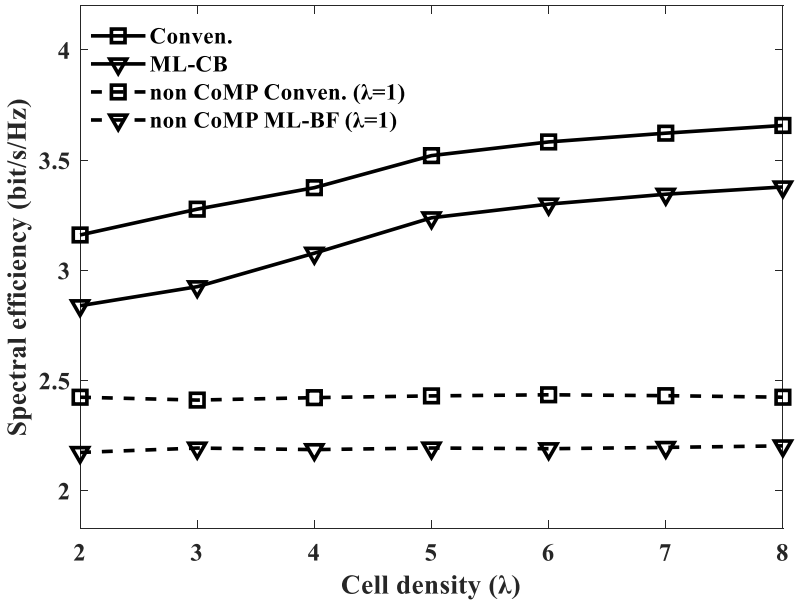

Figure 2. Spectral efficiency performance versus cell density.

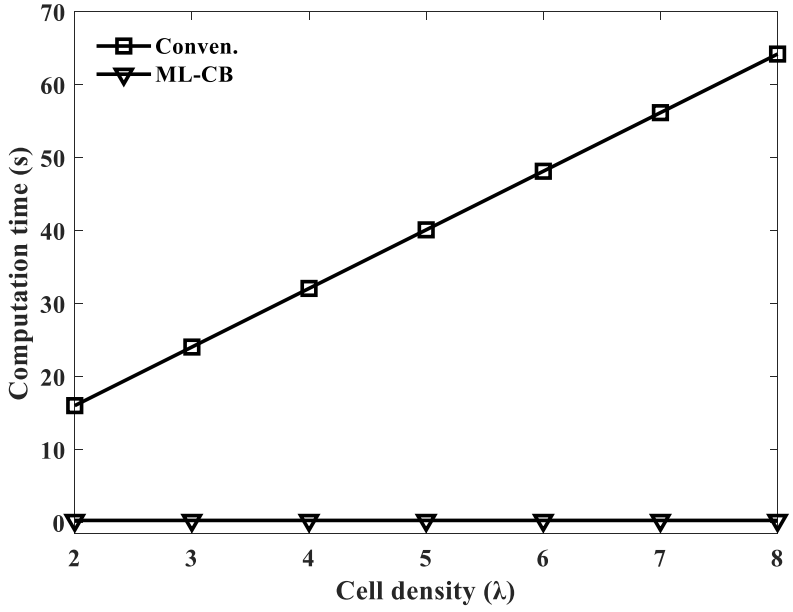

Figure 3. Computation times versus cell density.

4. Numerical Results and Discussion

In this section, we evaluate the performance of the proposed ML-CB-based massive MIMO system in UDN contexts. The spectral efficiency and computation times of conventional CB and the proposed ML-CB are compared.

The massive MIMO system and UDN context were designed in MATLAB® (R2018a). The Keras tool with a TensorFlow backend engine was used to implement the DNN models on a computer with an Intel® Core™ i7-8700 at 3.20 GHz, an NVIDIA GeForce RTX 2070, and 16 GB of memory. We considered a carrier frequency of 28 GHz and a system bandwidth of 100 MHz. All AUs were equipped with a 4×4 uniform rectangular array, and an MS with a single antenna was considered. We assumed a dense arrangement of small cells of 30-m radii. All the AUs of the small cells were at a distance of 20 m from the MS; that is: the AUs were placed at the vertices of a regular polygon, and the MS was located at its centre. The training and validation data sizes were approximately 51,000 and 9,000, respectively. A NR transmission frame was chosen and a subcarrier spacing of 60 kHz was considered in the 100 MHz band. One test data point was derived per RB, and 125 test data points were generated per subframe. The number of classes N_c^2 was 1,024, for an assumed 10-bit RF codebook. The measured mean absolute error of the DNN regressor was found to be 0.1067, and the training and validation accuracies of the DNN classifier were 95.83% and 94.76%, respectively.

Fig. 2 shows the spectral efficiency as a function of the cell density λ, for different beamforming schemes. The density indicates the number of small cells that can be connected to the MS. As shown, the ML-CB approach approaches the optimal performance, although there is some error in the prediction obtained by machine learning. The non-CoMP system results refer to a system in which the MS continues to be covered by a particular AU without multi-point cooperation. A non-CoMP ML based beamforming (ML-BF) represents the system with only the second stage applied. The obtained results show that in non-CoMP systems, the non-CoMP ML-BF can obtain a performance close to that of the non-CoMP conventional systems. These results show constant performance regardless of the cell density. In CoMP systems, higher spectral efficiencies can be obtained as the cell density increases, but the results show that the system performance starts to saturate gradually at $\lambda = 5$. This shows that there is a limit to the performance improvements obtained by increasing the cell density.

Fig. 3 shows the computation times of the conventional and ML-CB systems (the time required to determine the best serving cell and RF beam). To allow a fair evaluation of the computation time of both schemes, they were both processed using the GPU. In fact, the computation time using a CPU for the conventional scheme is similar to that using the GPU. In the conventional scheme, the computation time increases proportionally to the cell density. In contrast, the computation time of the ML-CB scheme is highly insensitive to cell density. At $\lambda = 2$ point, the computation time of conventional and ML-CB schemes is about 16s and 0.328s, respectively. This means that, when the conventional scheme is applied in our system, the beamformed downlink signal reaches its previous position when a pedestrian travelling at a speed of 3 km/h moves to a position 12.5 m away from the position which the uplink signal was transmitted. As the density of small cells increases, that gap widens. On the other hand, the ML-CB system can transmit the downlink signal when the pedestrian passes 0.272 m. This shows that the ML-based CB can guarantee low transmission delays and constitutes an essential approach, in terms of computation time, for the implementation of low-latency 5G UDNs.

5. Conclusion

In this study, we investigated an ML-based coordinated beamforming approach for millimetre-wave massive MIMO systems in UDN contexts. The CoMP approach can degrade system performance in an environment in which the number of small cells is larger than the number of MSs. To reduce the computation complexity for the coordinated beamforming, two DNN models are investigated. The proposed ML-CB can achieve coordinated beamforming with near-optimal performance and short computation times. It is efficient and easy to implement millimeter-wave MIMO systems in UDN. The proposed approach can also be applied

for fast and suitable beamforming and handover in various wireless communication fields including vehicle to infrastructure and massive machine type communications where UDN is considered. In future work, we will determine whether novel coordinated transmission processing schemes can be developed based on the proposed approach, for various interference environments.

Acknowledgement

This work was financially supported by the Research Year of Chungbuk National University in 2020.

References

[1] Ericsson: “Ericsson mobility report (Revision A),” 2019.
[2] P. Wang, Y. Li, L. Song, B. Vucetic, “Multi-gigabit millimeter wave wireless communications for 5G: from fixed access to cellular networks,” IEEE Commun. Mag., vol. 53, no. 1, pp. 168–178, 2015. DOI: https://doi.org/10.1109/MCOM.2015.7010531
[3] F. Sohrabi, W. Yu, “Hybrid digital and analog beamforming design for large-scale antenna arrays,” IEEE J. Sel. Topics Signal Process., vol. 10, no. 3, pp. 501–513, 2016. DOI: https://doi.org/10.1109/JSTSP.2016.2520912
[4] D. Lopez-Perez, M. Ding, H. Claussen, A. H. Jafari, “Towards 1 Gbps/UE in cellular systems: Understanding ultra-dense small cell deployments,” IEEE Commu. Surv. Tutor., vol. 17, no. 4, pp. 2078–2101, 2015. DOI: https://doi.org/10.1109/COMST.2015.2439636
[5] D. Lee, H. Seo, B. Clerckx, et al., “Coordinated multipoint transmission and reception in LTE-Advanced: deployment scenarios and operational challenges,” IEEE Commun. Mag., vol. 50, no. 2, pp. 148–155, 2012. DOI: https://doi.org/10.1109/MCOM.2012.6146494
[6] 3GPP, “Scenario and requirements for small cell enhancements for E-UTRA and E-UTRAN (Release 12),” 3GPP, Sophia Antipolis, France, Tech. Rep. TR 36.932 V12.1.0, 2013.
[7] V. Jungnickel, K. Manolakis, W. Zirwas, et al., “The role of small cells, coordinated multipoint, and massive MIMO in 5G,” IEEE Communications Magazine, vol. 52, no. 5, pp. 44–51, 2014. DOI: https://doi.org/10.1109/MCOM.2014.6815892
[8] M. Soltani, V. Pourahmadi, A. Mirzaei, H. Sheikhzadeh, “Deep learning-based channel estimation,” IEEE Commun. Lett., vol. 23, no. 4, pp. 652–655, 2019. DOI: https://doi.org/10.1109/LCOMM.2019.2898944
[9] H. Huang, Y. Song, J. Yang, G. Gui, F. Adachi, “Deep-learning-based millimeter-wave massive MIMO for hybrid precoding,” IEEE Trans. Veh. Technol., vol. 68, no. 3, pp. 3027–3032, 2019. DOI: https://doi.org/10.1109/TVT.2019.2893928
[10] S. Schwarz, C. Mehlfuhrer, and M. Rupp, "Calculation of the spatial preprocessing and link adaption feedback for 3GPP UMTS/LTE," in 6th conference on Wireless advanced (WiAD), IEEE, 2010. DOI: https://doi.org/10.1109/WIAD.2010.5544947
[11] 3GPP, “Physical channels and modulation (Release 15),” 3GPP, Tech. Spec. TS38.211, V15.0.0, 2017.
[12] 3GPP, “Study on channel model for frequencies from 0.5 to 100 GHz (Release 14),” 3GPP, Tech. Rep. TR38.901, V14.3.0, 2017.
[13] Y. Na, L. Zhang, X. Sun, “Efficient downlink channel estimation scheme based on block-structured compressive sensing for TDD massive MU-MIMO systems,” IEEE Wireless Commun. Lett., vol. 4, no. 4, pp. 345–348, 2015. DOI: https://doi.org/10.1109/LWC.2015.2414933
[14] B. Hochwald, T. Mazetta, T. Richardson, W. Sweldens, R. Urbanke, “Systematic design of unitary space-time constellations,” IEEE Trans. Inform. Theory, vol. 46, no. 6, pp. 1962–1973, 2000. DOI: https://doi.org/10.1109/18.868472

[15] D. Lee, H. Seo, B. Clerckx, E. Hardouin, D. Mazzarese, S. Nagata, and K. Sayana, "Coordinated Multipoint Transmission and Reception in LTE-Advanced: Deployment Scenarios and Operational Challenges," IEEE Communications Magazine, vol. 50, no. 2, pp. 148–155, Feb. 2012.
DOI: https://doi.org/10.1109/MCOM.2012.6146494

[16] D. Kingma, J. Ba, “ADAM: a method for stochastic optimization,” ICLR, 2015. [Online]. Available: https://arxiv.org/abs/1412.6980